OXFORD

Cerebral Cortex, November 2020;30: 5686–5701

doi: 10.1093/cercor/bhaa138
Advance Access Publication Date: 9 June 2020
Original Article

ORIGINAL ARTICLE

Evaluating the Sensitivity of Resting-State BOLD Variability to Age and Cognition after Controlling for Motion and Cardiovascular Influences: A Network-Based Approach

Peter R. Millar[1], Steven E. Petersen[1,2,3], Beau M. Ances[2,3], Brian A. Gordon[1,3], Tammie L. S. Benzinger[3], John C. Morris[2] and David A. Balota[1,2]

[1]Department of Psychological and Brain Sciences, Washington University in St. Louis, St. Louis, MO 63130, USA, [2]Department of Neurology, Washington University in St. Louis, St. Louis, MO 63130, USA and [3]Department of Radiology, Washington University in St. Louis, St. Louis, MO 63130, USA

Address correspondence to Peter R. Millar, One Brookings Drive, Campus Box 1125, St. Louis, MO 63130, USA. Email: pmillar@wustl.edu

Abstract

Recent functional magnetic resonance imaging (fMRI) studies report that moment-to-moment variability in the BOLD signal is related to differences in age and cognition and, thus, may be sensitive to age-dependent decline. However, head motion and/or cardiovascular health (CVH) may contaminate these relationships. We evaluated relationships between resting-state BOLD variability, age, and cognition, after characterizing and controlling for motion-related and cardiovascular influences, including pulse, blood pressure, BMI, and white matter hyperintensities (WMH), in a large ($N = 422$) resting-state fMRI sample of cognitively normal individuals (age 43–89). We found that resting-state BOLD variability was negatively related to age and positively related to cognition after maximally controlling for head motion. Age relationships also survived correction for CVH, but were greatly reduced when correcting for WMH alone. Our results suggest that network-based machine learning analyses of resting-state BOLD variability might yield reliable, sensitive measures to characterize age-related decline across a broad range of networks. Age-related differences in resting-state BOLD variability may be largely sensitive to processes related to WMH burden.

Key words: aging, BOLD variability, machine learning, resting-state fMRI

Introduction

Cognitive neuroscientists most often apply functional magnetic resonance imaging (fMRI) to analyze region-specific mean levels of task-related change or spontaneous correlation in the blood oxygen-level-dependent (BOLD) signal. These methods have provided valuable insight into in vivo human brain function and the intrinsic organization of brain networks (for review, see Fox and Raichle 2007). More recently, a growing body of research has begun to consider moment-to-moment variability in the BOLD signal over a given time-course as another potentially important measure of interest in cognitive neuroscience (for review, see Garrett, Samanez-Larkin, et al. 2013; Grady and Garrett 2014).

Specifically, BOLD variability appears to be sensitive to differences across the lifespan. Extreme groups comparisons between healthy younger and older adults have revealed widespread

patterns of age-related reduction in BOLD standard deviation (SD) during brief fixation blocks (Garrett et al. 2010), task performance (Garrett et al. 2011; Grady and Garrett 2018), and extended resting-state scans (Kielar et al. 2016; Grady and Garrett 2018). This general finding has been replicated in larger, continuous lifespan samples using other measures of BOLD signal variability, including fractional amplitude of low-frequency fluctuation (Hu et al. 2014) and mean square successive difference (Nomi et al. 2017). Although these studies often report negative relationships between age and BOLD variability broadly distributed throughout gray matter, likely spanning several networks, some sparser regional positive relationships are also observed within the same studies (e.g., Garrett et al. 2010; Nomi et al. 2017).

In addition to age, BOLD variability may also be related to cognition. This proposal is supported by task-driven fMRI studies demonstrating that greater BOLD variability is associated with faster, more accurate, and more consistent performance in a wide range of behavioral tasks, including simple motor responses, perceptual decision-making, spatial working memory, and trait judgments (Garrett et al. 2011; Guitart-Masip et al. 2016; Grady and Garrett 2018). Furthermore, potentially trait-like relationships have also been demonstrated between resting-state BOLD variability and cognitive measures acquired outside the scanner, including flanker task performance (Mennes et al. 2011) and factor scores of fluid intelligence and episodic memory (Burzynska et al. 2015b). Although, like the age difference relationships, some region-specific negative relationships between BOLD variability and behavior have been reported as well (Garrett et al. 2011; e.g., Burzynska et al. 2015b; Guitart–Masip et al. 2016).

Together, the negative relationships with age and positive relationships with behavior suggest that BOLD variability might reflect a sensitive brain signal that declines in older adults. The mechanism underlying these relationships, however, remains unclear. Some authors have proposed that BOLD variability may reflect a pattern of neural processing optimized for situations of environmental uncertainty (Grady and Garrett 2018). Under this view, a neural system that allows for ongoing exploration of potential activation states might afford optimal processing of unexpected stimuli and/or a more flexible set of responses (Deco et al. 2011). Others have suggested that greater dynamic range (observed as BOLD variability), particularly in network hubs, might afford efficient information processing within and between networks, thus supporting fluid cognitive abilities (Burzynska et al. 2015b). Other efforts have suggested possible links between BOLD variability and dopaminergic neuromodulation (Garrett et al. 2015; Guitart-Masip et al. 2016), a mechanism implicated more broadly in models of neurocognitive aging (Backman et al. 2006). Further work is necessary to disentangle these competing accounts and interrogate the mechanistic interpretation of BOLD variability. However, each of these interpretations assumes that BOLD variability reflects a true signal of neural processing. In the present report, we are agnostic to the specific mechanism and instead focus on methodological refinements to address the limitations of the previous work. These approaches might serve to test mechanistic accounts and evaluate potential clinical utility of resting-state BOLD variability measures in future studies of both health and disease. In this light, the present project has five distinct goals.

First, the influence of head motion and global signal artifact has not been well characterized in the previous literature on BOLD variability. In other areas of functional neuroimaging, particularly functional connectivity, there has been considerable interest in head motion (Power et al. 2012; Satterthwaite et al. 2012; Van Dijk et al. 2012). Consequently, the field has advanced through the development of principled methods to identify and control for motion-related confounds (Power et al. 2014, 2015). Indeed, head motion, heart rate variability, and respiratory variability have been shown to be positively associated with SD of the global resting-state BOLD signal, even after denoising via motion parameter, white matter, and cerebral spinal fluid (CSF) regression (Power et al. 2017). Furthermore, age is also positively associated with head motion, notably within BOLD variability datasets (e.g., Nomi et al. 2017). Hence, a priori one might expect that age-related differences in BOLD variability might actually increase with stricter motion control. This interpretation was supported by an early BOLD variability study, which reported that applying more "extended" preprocessing stages, including independent component analysis (ICA) denoising and regression of motion parameters, white matter, and CSF time series, resulted in both lower estimates of voxel-wise BOLD SD and stronger relationships between BOLD SD and age, as compared with "basic" preprocessing (Garrett et al. 2010). However, depending on the anatomical specificity and direction of these relationships, it is possible that motion and global signal artifacts might confound or obscure the effect of interest. In either case, careful parametric investigation of state-of-the art artifact rejection procedures should more systematically characterize the role of motion in BOLD variability estimates.

Second, some authors contend that resting-state BOLD variability may reflect vascular, rather than neuronal, factors. Indeed, there is evidence that age relationships with resting-state BOLD variability are reduced or eliminated after controlling for measures of cardiovascular health (CVH) and/or cerebral blood flow (Tsvetanov et al. 2015, 2019). However, it is also worth noting that one other study has observed consistent age relationships with resting-state BOLD variability after correcting for estimates of cerebral blood flow and cerebrovascular reactivity (Garrett et al. 2017). Hence, it is possible that changes in cardiovascular and neurovascular factors may contribute to age-related differences in resting-state BOLD variability. However, it is unclear whether cognitive relationships with BOLD variability may be similarly sensitive to vascular mechanisms. Indeed, there is emerging evidence that age-related disruptions in neuro-vascular coupling may contribute to reductions in neural efficiency and cognitive decline (for review, see Abdelkarim et al. 2019), but these influences have not been examined in the context of BOLD variability during resting-state or task performance. As previously described, relationships between resting-state BOLD variability and behavior are well documented, notably within samples of a limited age range of younger (Mennes et al. 2011) or older adults (Burzynska et al. 2015b)—samples which presumably should include a relatively limited range of CVH. Furthermore, in task-driven studies, BOLD variability has also been shown to modulate as a function of task difficulty within younger adult samples (Garrett et al. 2014), suggesting a possible link to cognitive demands. Hence, it is important to consider the extent to which vascular factors (here including measures of pulse, blood pressure, body mass index [BMI], and white matter hyperintensities [WMH]) might contribute to resting-state BOLD variability relationships with cognition, as well as with age. WMH may reflect progressive small vessel disease associated with CVH across the lifespan (Schmidt et al. 1999; Pantoni 2010), whereas other cardiovascular measures (i.e., pulse, blood pressure, BMI) may be more sensitive

to current CVH. However, it is also possible that WMH may also be sensitive to distinct pathological processes, including, for instance, traumatic brain injury (Marquez De La Plata et al. 2007) or multiple sclerosis (Filippi et al. 2011).

Third, regional specificity of BOLD variability relationships has most often been assessed in a voxel-wise manner or using a data-driven latent variable partial least squares approach (PLS, Krishnan et al. 2011). Since voxel locations are not constrained by underlying anatomical structure, these methods do not allow for the estimation of BOLD variability within anatomically distinct or functionally coherent regions (Wig et al. 2011). If resting-state BOLD variability is indeed an important property of the system, its relationships should be topographically organized in a meaningful structure, which can be observed in fMRI at the level of areas or networks. Organization at this level can be observed in voxel-wise patterns, but statistical thresholding procedures limit the interpretation of potentially informative marginal or trend-level network patterns. Furthermore, averaging estimates of BOLD variability within areas or networks should increase signal-to-noise ratio and mitigate the problem of multiple statistical comparisons, compared with a voxel-wise approach. Functional connectivity researchers have recognized these concerns in the context of defining network nodes (Wig et al. 2011) and have benefited from the development of ROI atlases dividing the brain into putative areas (Power et al. 2011; Yeo et al. 2011; Gordon et al. 2016). Additionally, the multivariate PLS approach can offer limited interpretability and is not as broadly used as other modeling procedures. Hence, in the present study, we will use an atlas-based ROI approach to study the anatomical patterns in resting-state BOLD variability at the level of areas and networks.

Fourth, evidence of age-related differences in BOLD variability comes mostly from studies with relatively small samples and extreme groups comparisons (but for exceptions, see Hu et al. 2014; Nomi et al. 2017). Hence, it is unclear whether BOLD variability is sensitive to continuous or more subtle age differences (e.g., middle age vs. older adulthood). This level of sensitivity would be useful if the estimates of BOLD variability are to be considered as potential biomarkers for distinguishing healthy aging trajectories from pathology, for example, Alzheimer disease. The present study explores a large sample of well-characterized, cognitively normal participants.

Fifth, and finally, the evaluation of BOLD variability as a potential clinically relevant signal might benefit from the application of multivariate, supervised machine learning techniques (for review, see Nielsen et al. in press). Specifically, methods such as support vector regression (SVR) afford prediction of continuous individual values (e.g., age or disease severity) based on multivariate inputs (e.g., region-specific patterns of BOLD variability or functional connectivity) using a model trained on separate observations. Machine learning methods have an applied advantage over regression approaches in that they assess and optimize the ability of a model to predict independent cases outside the observed training set, whereas regression models are limited to the fit of the model to the set of observed cases (Yarkoni and Westfall 2017). Hence, SVR would be useful to assess whether resting-state BOLD variability might serve as a generalizable biomarker of age-related or pathological processes. These methods have been recently applied to resting-state functional connectivity data, resulting in sensitive, continuous prediction of development (Nielsen et al. 2019). In the area of age-related decline, there is also a growing body of work using similar machine learning methods to predict age from functional and structural imaging measures (for review, see Cole and Franke 2017). Importantly, these studies have demonstrated that deviations from normative lifespan trajectories of these measures may be sensitive to neurodegenerative disease and cognitive decline. If resting-state BOLD variability is indeed a meaningful signal, it may yield unique clinical utility in this effort to identify biomarkers of healthy and early pathological changes.

The present study advances the study of resting-state BOLD variability by addressing each of the five topics discussed above. Specifically, we will characterize and maximally control for the influence of head motion and global signal-related effects on estimates of resting-state BOLD variability. We will also evaluate whether cardiovascular factors might contribute to relationships between resting-state BOLD variability, age, and cognition. Furthermore, we will examine these relationships at the level of putative brain areas and networks using an independently generated, network-based ROI atlas and will test age relationships with resting-state BOLD variability in a large sample of cognitively normal participants spanning a continuous age range from middle age to older adulthood. Finally, we will use a machine learning approach to evaluate the individual prediction accuracy of age and cognition from multivariate patterns of resting-state BOLD variability. This approach may contribute to the mechanistic understanding of resting-state BOLD variability by systematically addressing potential contaminating variables and evaluating network-level organization of these effects. Furthermore, our approach may advance potential clinical application by assessing and enhancing the reproducibility of resting-state BOLD variability analyses, as well as applying sensitive, multivariate predictive techniques to evaluate its utility as an age-related biomarker.

Materials and Methods

Participants

A sample of 422 older adult participants was selected from a larger set of participants enrolled in longitudinal studies at the Charles and Joanne Knight Alzheimer Disease Research Center at Washington University in St. Louis. The sample was selected on the basis of having a minimum value of usable resting-state fMRI data (see below), cognitive normality, as carefully assessed by trained clinicians using the Clinical Dementia Rating (Morris 1993), and absence of severe psychiatric conditions. See Table 1 for a summary of demographic and descriptive measures in the sample. A subset of participants ($N = 207$) had multiple longitudinal resting-state scan sessions available. Longitudinal scans occurred approximately once every 3 years. These longitudinal sessions were used only to assess test–retest reliability of resting-state fMRI measures. All procedures were approved by the Human Research Protection Office at Washington University in St. Louis. All participants provided informed consent prior to clinical assessment, psychometric testing, and neuroimaging.

Psychometric Battery

Participants completed a battery of psychometric tests. In order to investigate relationships between resting-state BOLD variability and global cognitive function, we examined performance on a subset of tasks across multiple cognitive domains, including measures of episodic memory (Free and Cued Selective Reminding Test [FCSR]: free recall score; Grober et al.

Table 1 Demographic, psychometric, and cardiovascular measures of the sample at four levels of motion censoring (mean FD > 0.20). MMSE = Mini Mental State Examination, BPM = beats per minute

	Measure (units)	Censor FD < 0.30			Censor FD < 0.20			Censor FD < 0.20, mean FD < 0.25			Censor FD < 0.20, mean FD < 0.20		
		N	Mean (SD)	Range	N	Mean (SD)	Range	N	Mean (SD)	Range	N	Mean (SD)	Range
Demographic	Age (years)	422	66.57 (8.73)	43–89	356	66.35 (8.92)	43–89	330	66.2 (9.01)	43–89	254	65.84 (9.05)	46–89
	Sex (*N* female/*N* male)	422	250/172	NA	356	213/143	NA	330	197/133	NA	254	150/104	NA
	Education (years)	422	15.92 (2.64)	6–20	356	15.94 (2.63)	6–20	330	15.95 (2.65)	6–20	254	15.90 (2.54)	10–20
	Race (*N* white/*N* black/*N* Asian)	422	385/35/2	NA	356	327/27/2	NA	330	303/25/2	NA	254	236/16/2	NA
	Mean head motion (mm FD)	422	0.19 (0.08)	0.05–0.49	356	0.17 (0.06)	0.05–0.31	330	0.16 (0.05)	0.05–0.25	254	0.14 (0.04)	0.05–0.2
Psychometric	MMSE (score)	351	29.13 (1.16)	23–30	300	29.14 (1.15)	24–30	279	29.12 (1.17)	24–30	214	29.14 (1.19)	24–30
	FCSRT: free recall (score)	396	31.17 (5.83)	4–46	336	31.28 (5.77)	4–46	311	31.2 (5.81)	4–46	240	31.32 (5.78)	14–46
	Animal naming (score)	397	21.91 (5.82)	8–41	337	21.9 (5.8)	8–41	312	21.92 (5.79)	8–41	241	21.88 (5.93)	9–41
	Trail making A (score)	397	30.62 (11.68)	10–134	337	30.39 (11.9)	10–134	312	30.37 (11.88)	10–134	241	29.85 (10.6)	10–69
	Trail making B (score)	396	75.68 (32.63)	19–234	336	75.34 (31.93)	19–210	311	75.81 (32.9)	19–210	240	74.95 (33.29)	19–210
Cardiovascular	Pulse (BPM)	417	68.35 (9.67)	40–108	351	68.29 (9.57)	41–108	325	68.18 (9.49)	41–108	249	67.94 (9.81)	41–108
	Systolic blood pressure (mmHg)	421	127.1 (16.07)	88–187	355	126.48 (15.73)	88–187	329	126.12 (15.69)	88–187	253	125.67 (15.62)	88–168
	BMI (kg/m^2)	421	26.91 (4.62)	14–42	355	26.5 (4.56)	14–41	329	26.3 (4.5)	14–41	253	26.14 (4.5)	14–41
	WMH volume (mm^3)	325	12 657.08 (16 214.36)	48–138 272	270	11 886.14 (14 670.1)	48–86 112	249	11 504.51 (14 254.41)	48–86 112	192	11 252.7 (13 918.06)	48–86 112

1988), semantic fluency (Animal Naming; Goodglass and Kaplan 1983), processing speed (Trail Making A, Armitage 1946), and executive function (Trail Making B, Armitage 1946). As shown in Supplementary Table 1, these measures were significantly correlated in the expected directions (absolute $rs = 0.24–0.56$, $Ps < 0.001$). As described previously (Aschenbrenner et al. 2018), each measure was standardized to the sample mean and SD. A global cognitive composite measure was calculated as the average across the standardized psychometric measures (after reverse-scoring the standardized Trail Making measures, which were based on completion time rather than correct responses).

CVH Measures

Following Tsvetanov et al. (2019), we attempted to form a composite of CVH. Measures of CVH included resting pulse, systolic blood pressure, and BMI. In addition, we included estimates of white matter hyperintensity (WMH) lesion volume. WMH volumes were assessed with a fluid-attenuated inversion recovery sequence, after segmentation using the Lesion Segmentation Tool (Schmidt et al. 2012) for SPM 8. We calculated a composite measure of CVH as the average of the standardized measures of pulse, systolic blood pressure, BMI, and WMH. However, as shown in Supplementary Table 2, correlations among the four measures were fairly small ($rs = -0.06–0.17$). Moreover, WMH volume stood out as having relatively strong relationships with both age ($r = 0.56$, $P < 0.001$) and resting-state BOLD variability ($r = -0.25$, $P < 0.001$), in comparison to the other CVH measures. Hence, we evaluated a global CVH composite (including WMH) and also a singular estimate of WMH. Importantly, the low correlations with other CVH measures suggest that WMH might capture specific variance within the sample that is not broadly related to general CVH.

Scanning Protocol and Preprocessing

MRI data were obtained using two separate Siemens Trio 3 T scanners equipped with a standard 12-channel head coil. A one-way analysis of variance revealed that there were significant age differences between the two scanners, $F = 6.53$, $P = 0.011$, raising the possibility that age differences in resting-state BOLD variability might be confounded by differences in the scanners. Thus, we replicated the results of our analyses of age effects after controlling for scanner as a factor of non-interest.

Structural and functional scans were acquired using methods described previously (Brier et al. 2012). Structural scans were acquired using a sagittal T_1-weighted magnetization-prepared rapid gradient echo sequence (MPRAGE; TR = 2400 ms, TE = 3.16 ms, flip angle = 8°, field of view = 256 mm, 1-mm isotropic voxels), as well as an oblique T_2-weighted fast spin echo sequence (FSE; TR = 3200 ms, TE = 455 ms, 256 × 256 acquisition matrix, 1-mm isotropic voxels). Resting-state functional scans were acquired using an interleaved whole-brain echo planar imaging sequence (EPI; TR = 2200 ms, TE = 27 ms, flip angle = 90°, field of view = 256 mm, 4-mm isotropic voxels). Participants completed two consecutive 6-min runs (164 volumes each) of functional imaging, during which they were instructed to stay awake and fixate on a visual crosshair.

Both resting state runs were processed together. Initial preprocessing followed conventional methods, as described previously (Shulman et al. 2010; Brier et al. 2012). Briefly, these steps included frame alignment correction for asynchronous

slice-time acquisition, debanding correction for interleaved slice intensities, rigid body transformation for motion correction within and across runs, bias field correction, and mode 1000 normalization. Transformation to an age-appropriate atlas template in 711-2B space was performed using composition of affine transforms connecting the functional volumes with the T_2-weighted and MPRAGE images. Head movement correction was included in a single resampling that generated a volumetric timeseries in isotropic 3-mm atlas space.

Additional processing was performed to allow for nuisance variable regression (Fox et al. 2009). First, masks of whole brain, gray matter, white matter, and CSF were generated from T_1 images in FreeSurfer (Fischl 2012). Second, two indices of framewise motion were calculated across the functional timeseries, including framewise displacement (FD; Power et al. 2012), which was based on the summed realignment estimates, and derivative of RMS variance over voxels (DVARS), which was based on framewise changes in signal intensity within the whole brain mask. Third, timeseries data were subjected to a temporal band-pass filter ($0.005 < f < 0.1$ Hz). Fourth, timeseries data were subjected to nuisance variable regression, including six motion parameters, as well as the timeseries estimates from the whole brain (global signal), CSF, ventricle, and white matter masks, as well as the derivatives of these signals. Finally, timeseries data were spatially blurred (6-mm full width at half maximum).

Preprocessed timeseries data were subjected to framewise censoring based on the motion estimates. Specifically, volumes were censored if they exceeded a threshold value of FD (we compared results from thresholds of 0.2 and 0.3 mm, see Results) or if DVARS was greater than 2.5 SD from the participant's mean value. Motion-related differences in the number of censored frames might confound the magnitude and/or reliability of BOLD variability estimates. Thus, we analyzed resting-state BOLD variability within a subset of 120 randomly selected usable frames from either run for each participant. Participants with fewer than 120 usable frames were excluded ($N = 21$).

Calculation of Resting-State BOLD Variability

Final timeseries data were averaged across voxels within a set of 298 ROIs from an expanded version of a previously defined atlas (Power et al. 2011; Seitzman et al. 2020), including 243 10-mm spheres in cortical areas, 28 8-mm spheres in subcortical areas, and 27 8-mm spheres in the cerebellum (see Seitzman et al. 2020, for a figure). Importantly, each of these ROIs has been assigned to one of 13 networks, including: somatomotor (SM), lateral somatomotor (SML), cingulo-opercular (CO), auditory (AUD), default mode (DMN), parietal memory (PMN), visual (VIS), fronto-parietal (FPN), salience (SAL), subcortical (SUB), ventral attention (VAN), dorsal attention (DAN), and cerebellum (CER). In each ROI, we calculated the SD of the BOLD signal over the 120 selected usable frames. These BOLD SD values served as our regional estimates of resting-state BOLD variability and as features in our machine learning analyses.

Support Vector Regression

SVR analyses were conducted using the e1071 package in R (Meyer et al. 2017). Briefly, SVR is a supervised machine learning technique in which a model is trained to identify multivariate relationships between a set of features (i.e., resting-state BOLD SDs in the 298 ROIs) and continuous labels (i.e., age, average head motion, or task performance). We performed epsilon-insensitive SVR, as described previously (Dosenbach et al. 2010; Nielsen et al. 2019). Briefly, in each training fold of epsilon-insensitive SVR, a regression line is fit in multivariate space between the feature set values and the label values. A tube of width *epsilon* is defined around the regression line. Data points outside this tube are penalized, while points inside the tube are not. The penalty factor C determines the trade-off between training error and model complexity. All SVR analyses were performed with epsilon = 0.00001 and C = infinity, based on previous reports predicting age from functional connectivity data (Dosenbach et al. 2010; Nielsen et al. 2019).

Importantly, the SVR model is trained on a subset of cases (the training set), allowing for the assessment of predictive accuracy of the model to generate labels based on the feature set in an unseen set of cases (the testing set). Specifically, we evaluated predictive accuracy using a 10-fold cross-validation procedure. For each of the 10 folds, a nonoverlapping set of 10% of the sample was set aside to serve as the testing set for that fold. The remaining 90% served as the training set for the multivariate model. Thus, across the 10 folds, the SVR model predicted a label value (e.g., model-predicted age) for each participant in the total sample. We assessed predictive accuracy of the model by computing the R^2 value, as well as the mean absolute error (MAE), between the model-predicted label values and the true label values for each participant.

Using these methods, we tested the predictive accuracy of SVR models trained on the full feature set of resting-state BOLD SD values from all 298 ROIs. Specifically, we tested the performance of these models to predict age, head motion, and cognitive function as labels of interest. Head motion labels were defined as mean FD observed in the resting-state scans, either before applying framewise censoring (precensored) or after (postcensored). Additionally, to assess whether resting-state BOLD SD could predict randomly selected values by capitalizing on noise, we attempted to predict a control label, defined as the original age values randomly permuted across participants in the sample (permuted age). Importantly, in order to characterize the influence of head motion on these relationships, we tested each SVR model across a parametric range of motion correction procedures. Specifically, we assessed relationships with resting-state BOLD SD in the following datasets, which represent increasingly conservative attempts to control for motion and global signal artifacts: 1) without nuisance regression or framewise censoring, 2) with nuisance regression and liberal framewise censoring (FD < 0.30), 3) with nuisance regression and conservative framewise censoring (FD < 0.20), 4) with nuisance regression and conservative censoring (FD < 0.20) within a restricted sample of participants with low head motion (mean FD < 0.25), and 5) with nuisance regression and conservative censoring (FD < 0.20) within a further restricted sample of participants with very low head motion (mean FD < 0.20).

Assessment of Network Specificity of Relationships

Anatomical specificity of relationships with resting-state BOLD SD at the level of networks was assessed in two ways. First, univariate regional correlations were calculated between the measure of interest and resting-state BOLD SD within each of the 298 ROIs, grouped by the functional network. Significance of network-level relationships with resting-state BOLD SD was tested using a bootstrap approach. Specifically, we randomly generated 10 000 bootstrap samples by resampling the

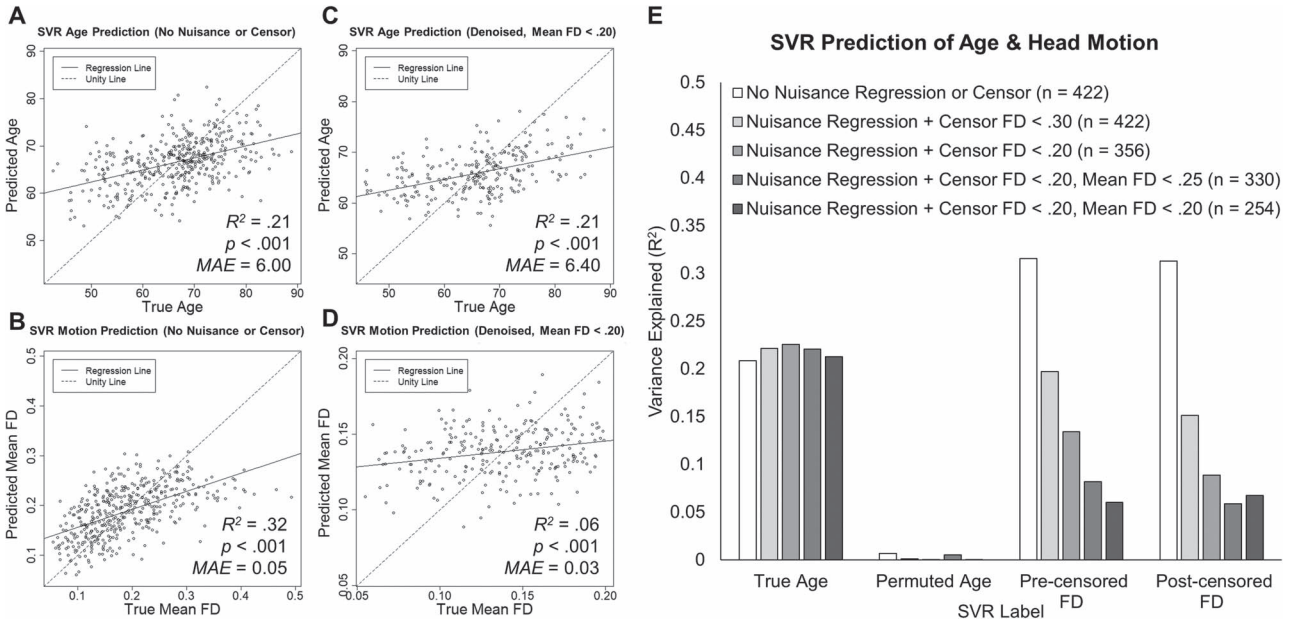

Figure 1. (*A–D*) SVR prediction results for age (*A* and *C*) and head motion (*B* and *D*). Label values predicted by the model are plotted as a function of the true value. SVR prediction results are displayed for resting-state BOLD SD values from data without nuisance regression or framewise censoring (*A* and *B*) and from the final denoised data (*C* and *D*). (*E*) SVR model prediction performance for true age labels, randomly permuted age, precensored FD, and postcensored FD across a range of artifact rejection procedures. Model prediction accuracy is plotted as variance explained, R^2, for each model.

full dataset with replacement. In each bootstrap sample, we calculated the correlation coefficient with the measure of interest in each ROI and then averaged the correlation values across ROIs within each network. Aggregating across bootstrap samples, we then calculated the empirical 95% confidence interval around the average correlation coefficient for each network.

Second, we also assessed the multivariate predictive accuracy of networks using modified SVR methods. Specifically, we used a network-based feature selection approach, in which we attempted to predict a measure of interest from a limited feature set of resting-state BOLD SD in regions restricted to a single network (e.g., only regions from the default mode network). Since larger networks should be biased to perform better simply due to a greater number of features, which might capture signal related to the variable of interest by chance, we compared SVR performance for network-specific feature sets to a bootstrapped distribution of 10 000 randomly selected feature sets (i.e., random regions from any network), which were matched in the number of total features. Hence, this bootstrapped distribution serves as an appropriate null model to test whether signals relating resting-state BOLD SD to a measure of interest are localized to specific networks or instead broadly distributed throughout the brain (Nielsen et al., in press).

Results

Reliability of Resting-State BOLD Variability

Since resting-state BOLD variability is a relatively underexplored fMRI measure, we first sought to examine the test–retest reliability of these estimates. One previous report has demonstrated that the estimates of BOLD SD exhibit excellent split-half reliability during resting fixation ($r = 0.97$) and task performance blocks ($rs = 0.91–0.95$; Garrett, Kovacevic, et al. 2013). Yet, we are unaware of any previous examinations of the reliability of BOLD variability across different sessions. Here, we assessed test–retest reliability of resting-state BOLD SD across relatively long intersession intervals (on average 3 years) among participants who were cognitively normal at both scans. Importantly, to compare their reliability against other established fMRI measures, we compared the estimates of resting-state BOLD variability (defined as average BOLD SD across all ROIs) to functional connectivity estimates from the same resting state fMRI dataset, including average intranetwork correlation values within each of the same networks (see Supplementary Fig. 1 for the resting-state correlation matrix). As shown in Supplementary Table 3 and Supplementary Figure 2, we observed fair test–retest correlation in resting-state BOLD SD over a 3-year interval ($r = 0.58$). Importantly, this reliability was better than or comparable to that observed for the established estimates of intranetwork functional connectivity (mean $r = 0.45$, range $= 0.30–0.60$). Of course, reliability of resting-state BOLD SD is important to know because the test–retest correlation sets a limit on how much variance can be accounted for by other variables of interest.

Influence of Motion Denoising on Sensitivity of Resting-State BOLD SD to Age and Motion

In order to characterize the influence of head motion on resting-state BOLD SD and its relationship with age, we evaluated the accuracy of SVR prediction for age and motion, based on multivariate feature sets of BOLD SD. Prior to advanced stages of motion denoising (nuisance regression and framewise censoring), resting-state BOLD SD was sensitive to age. As shown in Figure 1A, the SVR model was able to significantly predict participants' age based on BOLD SD inputs ($r = 0.46$, $P < 0.001$, $R^2 = 0.21$, MAE $= 6.00$), as expected considering previous demonstrations of this relationship (e.g., Garrett et al. 2010). However, in the same dataset, BOLD SD estimates were also highly sensitive to individual differences in mean head motion (see Fig. 1B;

$r = 0.56$, $P < 0.001$, $R^2 = 0.32$, MAE = 0.05). The multivariate pattern of resting-state BOLD SD explained a greater proportion of variance in head motion ($R^2 = 0.32$) than it did in age ($R^2 = 0.21$), suggesting that age-related variance in resting-state BOLD SD might be contaminated by differences in head motion in this sample. Indeed, age was positively associated with head motion, $r = 0.10$, $P = 0.03$.

We then assessed the extent to which head motion influenced the relationship between age and resting-state BOLD SD by maximally controlling for motion and global signal artifacts via nuisance regression (including global signal regression), framewise censoring, and exclusion of high-motion participants, which reduced the sample to 254 usable participants. After these conservative controls for motion, the sensitivity of resting-state BOLD SD to age replicated with roughly the same effect size (see Fig. 1C; $r = 0.46$, $P < 0.001$, $R^2 = 0.21$, MAE = 6.40). In contrast, the variance in head motion explained by resting-state BOLD SD was drastically reduced (see Fig. 1D; $R^2 = 0.06$, MAE = 0.03), although prediction of motion was still statistically significant ($r = 0.25$, $P < 0.001$).

To parametrically characterize the effectiveness of denoising procedures, we examined similar SVR model predictions from intermediate stages of preprocessed resting-state BOLD SD feature sets. As shown in Figure 1E, even after nuisance regression and relatively liberal framewise censoring (FD < 0.30), BOLD SD was still sensitive to head motion ($r = 0.44$, $P < 0.001$, $R^2 = 0.20$, MAE = 0.06), with a similar effect size to that observed for age in the same dataset ($r = 0.44$, $P < 0.001$, $R^2 = 0.22$, MAE = 6.23). However, with increasing control for motion, including a stricter framewise censoring threshold (FD < 0.20) and exclusion of participants with very high (FD > 0.25) or high (FD > 0.20) head motion, motion-related variance in resting-state BOLD SD steadily declined, while the sensitivity to age remained consistently high (see Fig. 1E). These patterns were similar for the measures of head motion calculated before or after framewise censoring. Although these stricter motion controls necessarily result in smaller sample sizes (i.e., Ns = 422 vs. 254), it is unlikely that the reduction in sensitivity to motion was driven by limited statistical power, as the sensitivity to age remained robust in the same restricted samples. Moreover, SVR prediction of permuted age was consistently low in all datasets, suggesting that the other models capture meaningful relationships with age and motion, rather than simply explaining random variance by chance. Altogether, these results clearly indicate that resting-state BOLD SD is influenced by head motion in relatively noisy data and that conservative methods of motion control are effective in minimizing this influence. Importantly, the sensitivity of resting-state BOLD SD to age remains robust across increasingly conservative motion denoising procedures.

Anatomical Specificity of Age and Motion Relationships with Resting-State BOLD SD

We then assessed whether age and motion were related to resting-state BOLD SD in specific networks by examining regional correlation patterns, grouped by network assignment. As shown in Figure 2A, we found surprisingly positive relationships between age and resting-state BOLD SD before motion denoising. These relationships were most prominent in the subcortical, cerebellum, and default mode networks, as well as unassigned regions, but marginal positive relationships were also observed in fronto-parietal and salience networks. These relationships are surprising considering previous reports of negative relationships between age and BOLD variability during resting-state or task performance (e.g., Garrett et al. 2010). As shown in Figure 2A, we only observed marginal negative relationships with age in the visual network. However, there were also very strong relationships between resting-state BOLD SD and head motion in these minimally processed data. As shown in Figure 2B, positive relationships were observed between motion and resting-state BOLD SD in all networks. Considering that age was positively associated with head motion in this sample, it is likely that motion-related increases in resting-state BOLD SD might positively bias relationships with age. Indeed, after applying conservative motion correction techniques, relationships between age and BOLD SD were more robustly negative. As shown in Figure 2C, negative relationships between age and resting-state BOLD SD were observed in all networks, except ventral attention, cerebellum, and unassigned regions. Importantly, relationships with head motion were greatly reduced in this dataset, as compared with the minimally processed results (see Fig. 2B,D), although positive relationships with motion were still observed in most networks consistent with prior work (Power et al. 2017).

Additionally, we assessed whether the multivariate age-related signal in resting-state BOLD SD might be unique to specific networks using network-based SVR feature selection. As shown in Figure 3, SVR predictions of age became more accurate as the number of randomly selected features increased (gray dots). This pattern is not surprising, considering that larger feature sets might capture more age-related signal by chance, resulting in better prediction, but importantly, it also establishes an appropriate null model to compare age prediction in specific networks. We found that SVR accuracy in network-specific models out-performed matched random feature sets in the subcortical network ($R^2 = 0.15$, empirical $P = 0.009$), ventral attention network ($R^2 = 0.04$, $P = 0.019$), and marginally in the parietal memory network ($R^2 = 0.02$, $P = 0.045$). Hence, there may be specific multivariate relationships between age and resting-state BOLD SD in these networks. In contrast, other networks fell within the range expected by randomly selected feature sets. Although there may be age-related signal in resting-state BOLD SD within these networks, this finding suggests that these networks offer no more sensitivity to age than can be achieved by randomly selecting regions independent of network assignment. Hence, the age-related signal is likely spread diffusely across these networks.

Relationships with Global Cognitive Function

In the denoised BOLD SD dataset, we tested whether resting-state BOLD SD was also sensitive to cognitive function measured outside the scanner. As shown in Figure 4A, we observed marginal positive relationships between cognitive composite scores and resting-state BOLD SD in parietal memory, visual, fronto-parietal, and dorsal attention networks (see Supplementary Material for "Analyses of Individual Neuropsychological Test Scores" and Supplementary Figure 3). These results are consistent with previous reports of positive relationships between BOLD variability and cognitive measures acquired both inside (Garrett et al. 2011; Guitart-Masip et al. 2016; Grady and Garrett 2018) and outside the scanner (Mennes et al. 2011; Burzynska et al. 2015b). Furthermore, as shown in Figure 4B, multivariate patterns in resting-state BOLD SD across networks captured a small, but significant, portion of variance in global cognitive ability ($r = 0.22$, $P < 0.001$, $R^2 = 0.05$, MAE = 0.58). However,

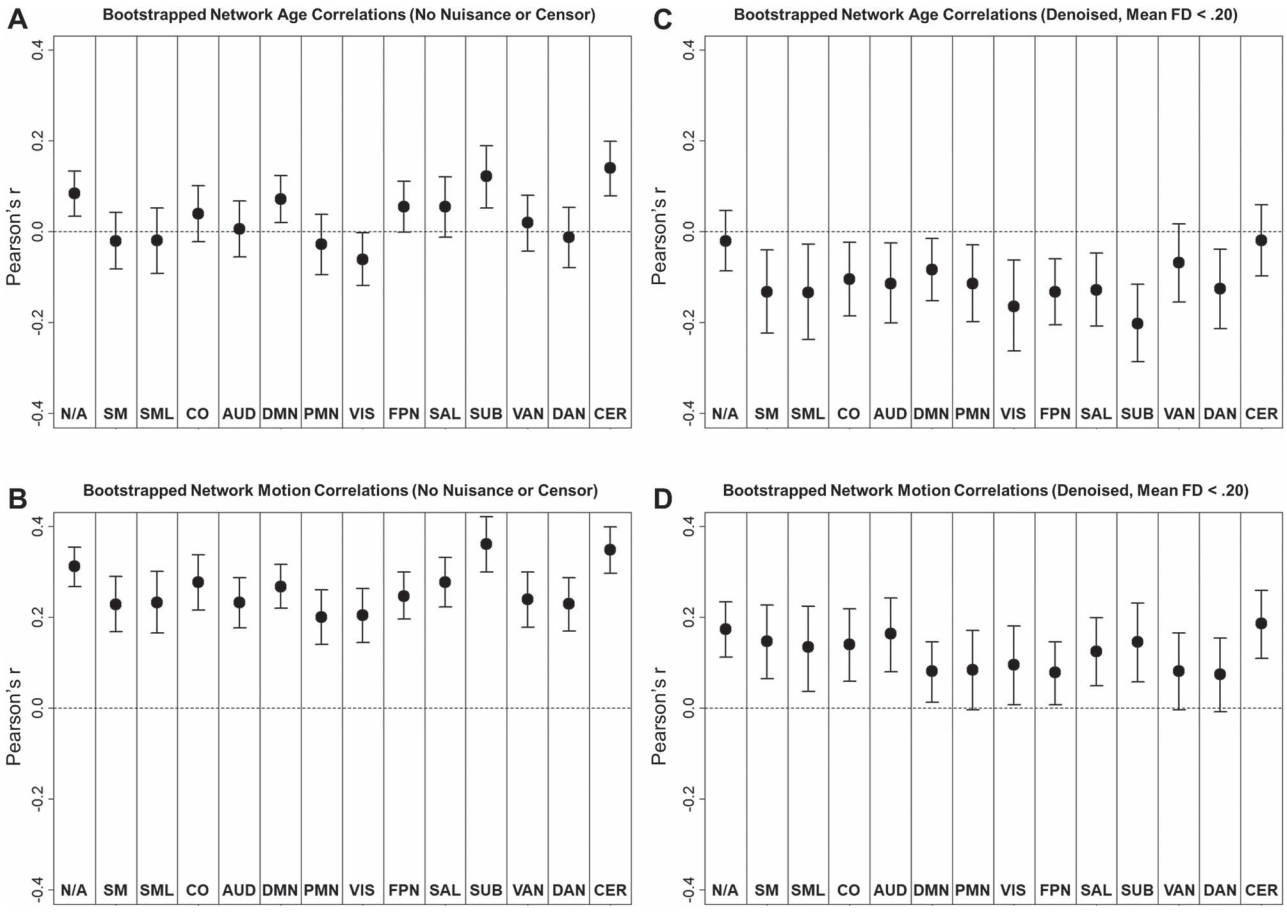

Figure 2. Network average Pearson correlations (bootstrapped mean and 95% confidence interval) between resting-state BOLD SD and age (*A* and *C*) or head motion (*B* and *D*).

these relationships did not replicate after controlling for age. As shown in Figure 4C, there were no significant relationship between global cognition and residual resting-state BOLD SD in any network after controlling for age. Furthermore, SVR models were unable to predict global cognitive ability from the residualized estimates ($r = -0.07$, $P = 0.272$, $R^2 = 0.01$, MAE = 0.62). Thus, resting-state BOLD SD was not related to global cognition above and beyond age differences.

Relationships with CVH and WMH

We also tested whether resting-state BOLD SD was sensitive to cardiovascular measures. As shown in Figure 5A, we observed negative relationships between CVH composite scores and resting-state BOLD SD in visual and subcortical networks. However, as shown in Figure 5C, multivariate patterns in resting-state BOLD SD across networks only captured a small, marginally significant portion of variance in CVH ($R^2 = 0.01$, $P = 0.065$, MAE = 0.40). In contrast, WMH volume alone was highly sensitive to resting-state BOLD SD. As shown in Figure 5B, we observed significant negative relationships between WMH and resting-state BOLD SD in all networks, except lateral somatomotor, ventral attention, and cerebellum. Furthermore, as shown in Figure 5D, multivariate patterns in resting-state BOLD SD captured a small, but significant, portion of variance in WMH ($R^2 = 0.07$, $P < 0.001$, MAE = 9510.16). See Supplementary Material for "Analyses of Individual CVH Measures" (Supplementary Figs 4 and 5), as well as "Principal Component Analyses of CVH Composite Measures" (Supplementary Table 4 and Supplementary Figs 6 and 7).

Relationships with Age and Cognition after Controlling for Cardiovascular Measures

Finally, we explored whether resting-state BOLD variability relationships with age and global cognition might be sensitive to cardiovascular factors. To examine this possibility, we attempted to replicate the previously established relationships with age and cognitive composite using residual estimates of resting-state BOLD SD after controlling for either the CVH composite or WMH volume in linear regression models.

Importantly, age relationships with resting-state BOLD variability survived the correction for the CVH composite. As shown in Figure 6A, we replicated the pattern of significant negative relationships between resting-state BOLD SD and age, observed in all networks, except for ventral attention, cerebellum, and unassigned regions. Furthermore, SVR models successfully predicted age from resting-state BOLD SD, even after controlling for CVH and maximally controlling for motion and global signal artifacts ($R^2 = 0.06$, $P < 0.001$, MAE = 6.65). In contrast, age relationships with resting-state BOLD SD did not survive the

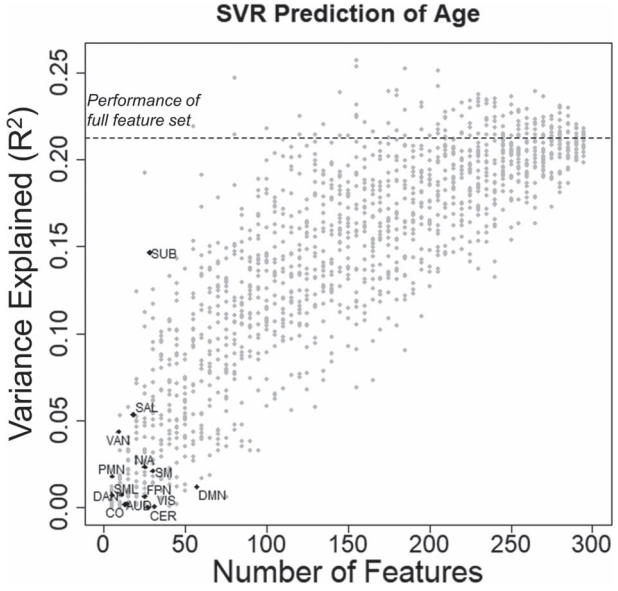

Figure 3. Performance of SVR models predicting age from denoised resting-state BOLD SD across a range of feature sets (from 5 to 295). Black diamonds denote anatomical feature selection schemes, in which features included only ROIs from a specific network (diamond labels). Each network-specific model was compared to 10 000 simulated models using randomly selected feature sets from any network. For simplicity, only 25 of the simulated models are plotted for each feature set size (gray dots).

correction for WMH volume. As shown in Figure 6B, we observed trend-level negative relationships between resting-state BOLD SD and age in most networks; however, none of these individual relationships reached significance. Moreover, SVR models did not successfully predict age from resting-state BOLD SD after controlling for WMH ($R^2 = 0.00$, $P = 0.977$, MAE = 7.37). Having said this, it is noteworthy that by a one-tailed binomial test, the observation of 12 or more negative trends in the 14 networks reliably differed from chance, $P = 0.006$.

In contrast to age relationships, cognitive relationship with resting-state BOLD variability did not survive correction for either CVH or WMH. As shown in Figure 6C, we observed some positive, marginal relationships with cognitive composite scores after controlling for CVH, but SVR models did not successfully predict cognition in these residualized data ($R^2 = 0.007$, $P = 0.279$, MAE = 0.56). After controlling for WMH, we observed no relationships with cognitive composite scores (see Fig. 6D) nor did SVR models successfully predict cognition ($R^2 = 0.004$, $P = 0.402$, MAE = 0.56).

Discussion

Our results offer several noteworthy findings. To review, we replicated previous reports that resting-state BOLD variability is negatively associated with age and positively associated with cognition. Furthermore, although head motion was shown to influence the estimates of resting-state BOLD variability, we observed relationships with age and cognition after applying maximally conservative artifact rejection procedures. However, resting-state BOLD variability was also marginally sensitive to CVH and particularly sensitive to WMH. Importantly, the negative relationship between age and resting-state BOLD variability was observed after controlling for a CVH composite, but was largely attenuated after controlling for WMH volume. We now discuss each of these findings in turn, focusing on their relevance in the context of previous reports, implications for the interpretation of resting-state BOLD variability as a signal of interest, and potential for application as a clinically relevant biomarker.

Relationships of Resting-State BOLD Variability with Age and Cognition

As expected from a growing body of reports, we observed that resting-state BOLD variability was sensitive to age. Although these effects have previously been demonstrated in extreme groups age comparisons (e.g., Garrett et al. 2010) or continuous lifespan samples (e.g., Nomi et al. 2017), here, we demonstrate that resting-state BOLD variability is sensitive to relatively subtle age differences, ranging continuously from middle age to older adulthood (43–89). This degree of age sensitivity might offer some clinical utility. Specifically, if continuous lifespan trajectories of resting-state BOLD variability can be well characterized in healthy samples, deviations from these trajectories might be interpreted as early markers of pathological processes.

In terms of network specificity, we observed negative relationships with age in a broad range of sensory (auditory, visual), motor (somatomotor), and association (cingulo-opercular, default mode, parietal memory, fronto-parietal, salience, dorsal attention) networks. Furthermore, network-driven feature selection revealed that SVR prediction of age based on resting-state BOLD variability features within most networks performed no better than randomly selected feature sets. These findings suggest that age-related signal in resting-state BOLD variability is broadly distributed throughout networks with little anatomical specificity. This pattern is fairly similar to widespread network differences in functional connectivity across development (Nielsen et al. 2019).

One noteworthy exception to this widespread pattern was the subcortical network. Indeed, we observed particularly strong negative relationships with age in subcortical regions. This pattern is surprising, as there is some inconsistency among previous reports of age relationships with resting-state BOLD variability in subcortical areas—including some reports of positive age relationships with resting-state and task-driven BOLD variability in striatum, thalamus, caudate, and putamen (Garrett et al. 2010; Garrett et al. 2011; Guitart-Masip et al. 2016). In fact, some researchers have proposed an anatomical-based framework in which BOLD variability in neocortical regions may decrease in advanced aging, while subcortical variability may increase (Garrett, Samanez-Larkin, et al. 2013; Guitart-Masip et al. 2016). Hence, the inverse subcortical age relationships in the present study are somewhat unexpected in light of these previous findings. In contrast, the results are more consistent with other findings that age is negatively associated with resting-state BOLD variability in thalamus and basal ganglia (Nomi et al. 2017). Notably, the report of negative subcortical age relationships from Nomi et al. (2017) tested age effects continuously in two overlapping, large datasets (*Ns* = 191, 187), in contrast to the smaller, extreme groups designs (Garrett et al. 2010; Garrett et al. 2011; Guitart-Masip et al. 2016). One possible account for this age relationship in subcortical regions may be that these areas are particularly susceptible to microvascular pathology, due to their proximity to vascular territories (for review, see Wardlaw et al. 2013). Indeed, we observed that WMH burden was also associated with resting-state BOLD SD in subcortical regions. For

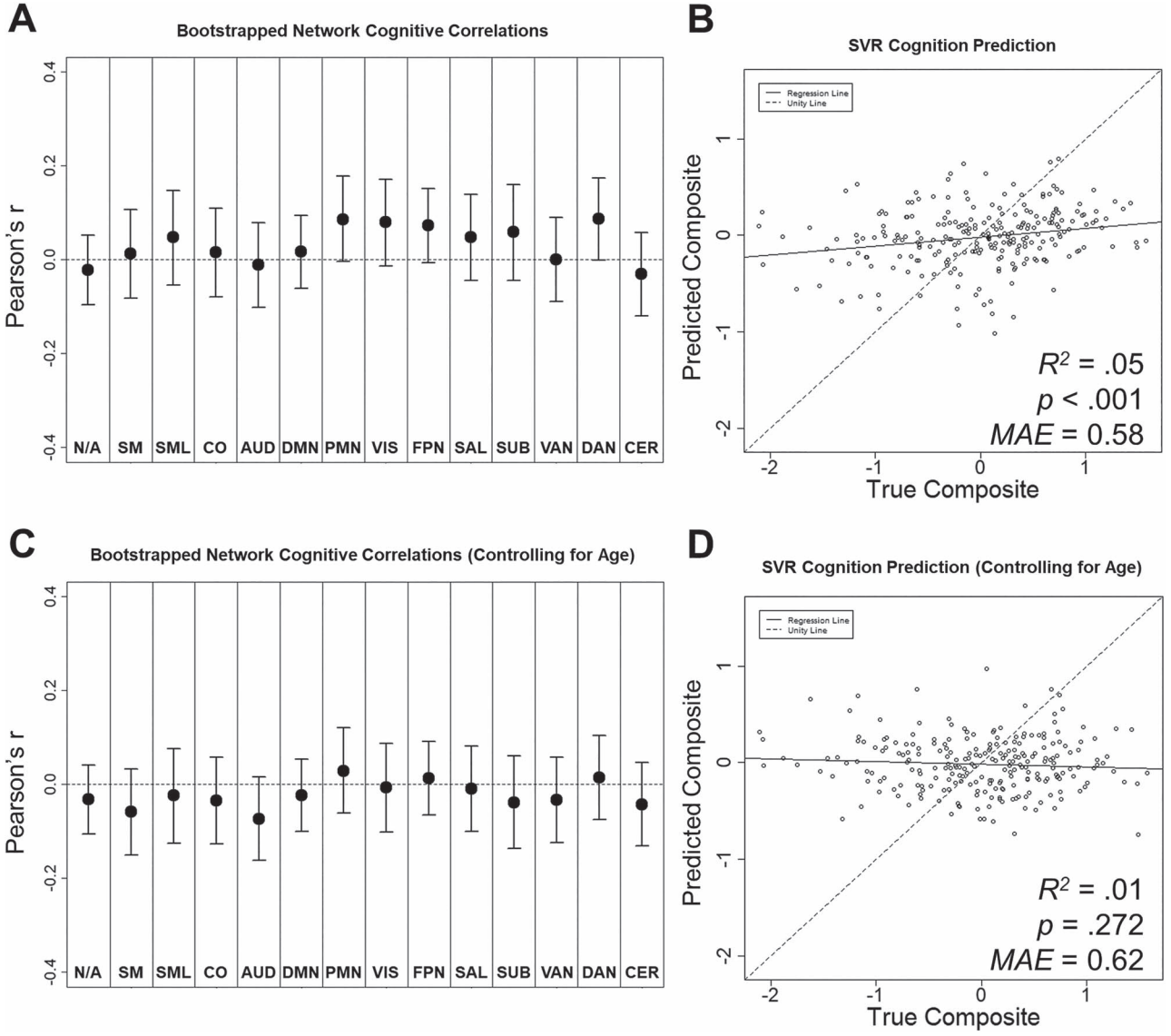

Figure 4. Relationships between resting-state BOLD SD and cognitive composite before (*A* and *B*) and after controlling for age differences (*C* and *D*). (*A* and *C*) Network average Pearson correlations (bootstrapped mean and 95% confidence interval) between resting-state BOLD SD and cognitive composite score. (*B* and *D*) Cognitive composite scores predicted by SVR model as a function of true score.

further examination of consistency in the topological patterns of resting-state BOLD SD in relation to age, motion, and WMH, see the Supplementary Material for "Consistency of SVR Weights Across Models" (Supplementary Figs 8 and 9)

We also replicate previous findings that resting-state BOLD variability is sensitive to cognitive measures assessed outside the scanner, including factor scores of fluid intelligence and episodic memory (Burzynska et al. 2015b), as well as flanker task performance (Mennes et al. 2011). Here, we extend upon these findings using a global cognitive composite of processing speed, executive function, episodic memory, and semantic fluency measures. These relationships were observed in visual, parietal memory, frontoparietal, and dorsal attention networks. However, compared with age relationships (SVR $R^2 = 0.21$), relationships between resting-state BOLD variability and cognition were relatively small (SVR $R^2 = 0.05$). Moreover, cognitive relationships were not observed after correcting for individual differences in age. Thus, the current analyses suggest that resting-state BOLD SD may only be related to cognition to the extent that it is sensitive to more general age-related differences. As suggested by our analyses with CVH measures, it is possible that these relationships may be particularly sensitive to WMH-related pathology. This finding is in agreement with demonstrations that cerebral small vessel disease is an important contributor to cognitive decline (for review, see Wardlaw et al. 2013).

Influence of Head Motion on Resting-State BOLD Variability

We observed that, similar to established influences on functional connectivity estimates (Power et al. 2012; Satterthwaite et al. 2012; Van Dijk et al. 2012), head motion and/or global signal artifacts were strongly related with resting-state BOLD variability in all networks. However, these relationships consistently declined as we applied increasingly conservative

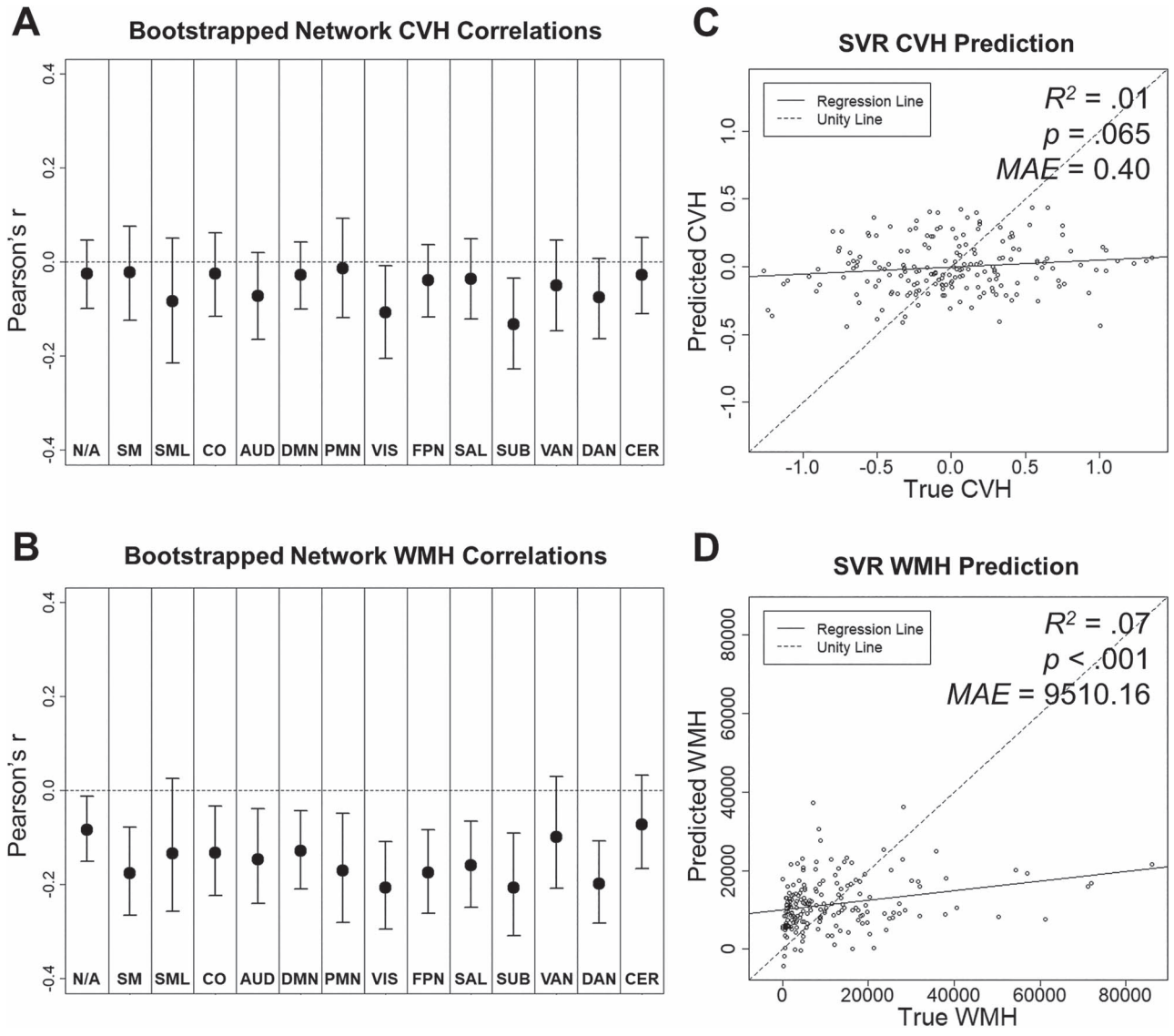

Figure 5. Relationships between resting-state BOLD SD, CVH composite (*A* and *C*), and WMH (*B* and *D*). (*A* and *B*) Network average Pearson correlations (bootstrapped mean and 95% confidence interval). (*C* and *D*) CVH and WMH measures predicted by SVR model as a function of true score.

artifact rejection procedures, including global signal regression, framewise censoring, and sample restriction. Yet, even in the most conservative dataset, we observed significant (although drastically reduced) relationships between resting-state BOLD SD and motion. These relationships are not particularly surprising, considering that motion has previously been shown to increase SD in the global resting-state BOLD signal, even after applying common motion correction techniques (Power et al. 2017). Thus, head motion may continue to positively bias estimates of resting-state BOLD variability, even in relatively "clean" samples.

Importantly, the degree to which researchers control for motion-related influence on resting-state BOLD variability may influence the size and direction of the relationships with age. Specifically, before applying nuisance regression and framewise censoring, we found that age was either unrelated or positively related with resting-state BOLD SD in most networks, with the possible exception of the visual network. These patterns would be expected if age-related increases in head motion positively bias estimates of resting-state BOLD variability in older adults. Indeed, older adults did have higher estimates of motion in our sample. However, after applying conservative methods to limit the influence of motion, we observed the expected robust inverse age relationships with resting-state BOLD variability. This pattern is more consistent with previous reports, which typically include some extended preprocessing procedures to correct for motion, including nuisance regression and ICA denoising (Garrett et al. 2010; Nomi et al. 2017), although these methods alone have been shown to be insufficient for removing motion-related and global signal artifacts in functional connectivity estimates (Ciric et al. 2017). This pattern aligns with an early report by Garrett et al. (2010), suggesting that more extended motion correction results in both lower estimates of resting-state BOLD variability and stronger relationships with age. Altogether, these findings suggest that motion correction procedures should be an important consideration when analyzing and interpreting age-related differences in resting-state BOLD variability.

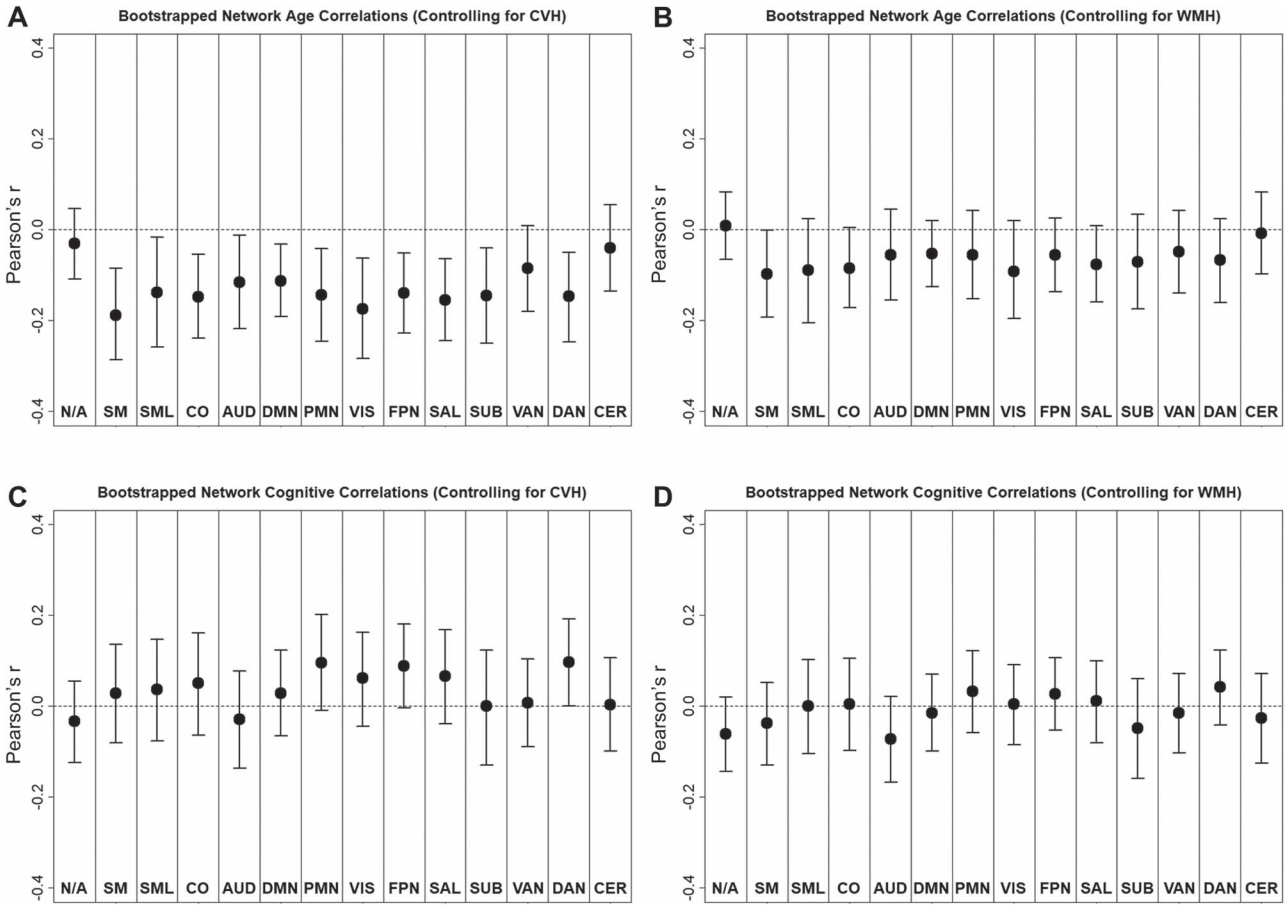

Figure 6. Network average Pearson correlations (bootstrapped mean and 95% confidence interval) between resting-state BOLD SD and age (*A* and *B*) or cognitive composite (*C* and *D*). Relationships are shown for residuals of resting-state BOLD SD after controlling for either the CVH composite (*A* and *C*) or WMHs (*B* and *D*).

Influence of CVH and WMH on Resting-State BOLD Variability

Turning to the influence of CVH and WMH on estimates of resting-state BOLD variability, we found that WMH volume was negatively related to variability throughout a wide range of networks. This relationship would be expected if reduced resting-state BOLD variability is indeed a marker of advancing cardiovascular or neurodegenerative pathology. This result contrasts with some recent studies, which have reported positive relationships between WMH volume and resting-state BOLD SD in parahippocampal gyrus, as well as temporal, frontoparietal, and orbitofrontal regions (Scarapicchia et al. 2018, 2019). However, it is worth noting that these relationships were observed in much smaller samples (Ns = 19 controls) than the current study ($N = 192$ participants with WMH in the final sample). Moreover, in one report, positive relationships with WMH only reached marginal trend-level significance ($P < 0.10$; Scarapicchia et al. 2018).

Importantly, after controlling for WMH, age relationships with resting-state BOLD variability were largely attenuated. This finding is partially consistent with a recent proposal that age-related differences in resting-state BOLD variability might be mediated by a combination of cardiovascular and neurovascular factors (Tsvetanov et al. 2019). However, in contrast to the results reported by Tsvetanov et al. (2019), we found that only controlling for WMH volume alone was necessary to attenuate the age relationship. Age relationships with resting-state BOLD SD were still observed after controlling for a CVH composite, which included measures of pulse, systolic blood pressure, and BMI, as well as WMH. Moreover, WMH volume was only modestly correlated with other measures in the CVH composite. Although somewhat surprising, these observations suggest that age-related variance in resting-state BOLD SD may be associated with WMH-specific pathology, rather than CVH in general. Importantly, although WMH should be related to CVH, WMH should not be interpreted as simply a proxy for CVH in the current sample. It is possible that WMH may reflect cumulative lifetime injury related to cardiovascular disease, as opposed to current CVH status, which may be better captured by other measures (e.g., blood pressure). Furthermore, as noted earlier, it is also worth noting that WMH may additionally be sensitive to traumatic brain injury (Marquez De La Plata et al. 2007) or other disease processes, including multiple sclerosis (Filippi et al. 2011).

These inconsistent findings may be attributed to sample- or method-related differences. Specifically, since our study examined a relatively narrow age range of middle-aged to older adults (43–89), we may observe a relatively restricted range of CVH, as compared with the adult lifespan sample (18–88) reported by Tsvetanov et al. (2019). Also, overall levels of WMH were relatively low in the current sample, due to screening of the

cohort, and thus, these results might not be representative of a population with greater vascular risk. Finally, the CVH composite used in the current study was formed using fewer available measures and used simple a priori averaging, rather than the data-driven factor analysis used by Tsvetanov et al. (2019), but see the Supplementary Material for "Principal Component Analyses of CVH Composite Measures" (Supplementary Table 4, Supplementary Figs 6 and 7).

Although age relationships with resting-state BOLD variability did not reach statistical significance after controlling for WMH, it is noteworthy that we observed nonsignificant negative trends in the same networks where significant age relationships were formerly observed. Indeed, a binomial test of the likelihood of observing 12 or more negative trends in the 14 networks revealed that this pattern was highly unexpected by chance, $P = 0.006$. Hence, there may be some meaningful negative relationship between age and resting-state BOLD variability below the level of statistical significance, even after controlling for WMH volume.

It is possible that the influence of WMH-related pathology may extend to other age-dependent imaging measures, beyond resting-state BOLD variability. For instance, there are well-established negative relationships between age and estimates of within-network functional connectivity (Betzel et al. 2014; Chan et al. 2014). As shown in Supplementary Table 5, we replicated the negative relationships between age and within-network functional connectivity in most networks when conservatively controlling for motion and global signal artifacts (mean $r = -0.15$, range $= -0.23$ to -0.02). Importantly, these relationships were reduced after controlling for WMH (mean $r = -0.06$, range $= -0.17$ to .09). Hence, similar to resting-state BOLD SD, it appears that fMRI-based estimates of functional connectivity might also be sensitive to age-related WMH pathology in carefully screened cognitively normal adults, similar to effects demonstrated using pulse and heart rate variability (Geerligs et al. 2017).

The influence of WMH on age-related differences in resting-state BOLD variability and functional connectivity might offer insight into the theoretical understanding of these measures. Specifically, low-frequency resting-state BOLD fluctuations might be the outcome of spontaneous activity within a differentially connected network of nodes (Honey et al. 2007). Under this framework, disruptions in the network structure might produce reductions in both the amplitude of these fluctuations and the magnitude of correlations among the fluctuations. Thus, to the extent that WMH lesions observed in the current sample disrupt white matter connections and network structure, these changes might be observed as reductions in both resting-state BOLD variability and functional connectivity. In this view, resting-state BOLD variability and functional connectivity might each reflect the outcomes of the same underlying age-related and pathological processes. Future studies might investigate similarities between age-related differences in resting-state BOLD variability and functional connectivity and test whether they might emerge from shared mechanisms.

Potential Clinical Utility of Resting-State BOLD Variability

Using a supervised, multivariate machine learning approach, we were able to successfully generate predictions about clinically relevant, continuous measures, including age, cognitive composite score, and WMH volume, in untrained observations. This demonstration suggests that resting-state BOLD variability might serve as a sensitive, generalizable biomarker of age-related decline, extending upon recent work using machine learning techniques to establish age-related biomarkers in structural MRI and functional connectivity measures (for review, see Cole and Franke 2017). Future machine learning analyses should assess whether resting-state BOLD variability (or deviations in normative age trajectories in resting-state BOLD variability) may successfully predict early neurodegenerative pathology, for example, Alzheimer disease.

Limitations and Future Directions

Although we demonstrated that WMH burden was related to resting-state BOLD variability and may influence relationships with age, we are limited in our ability to interpret the mechanisms underlying these relationships. As mentioned, WMH are associated with a range of pathological processes and were highly correlated with age in the current sample. These relationships might be sensitive to cardiovascular and/or metabolic factors (Alfaro et al. 2018). Alternatively, WMH may be sensitive to co-occurring neurodegeneration (Wardlaw et al. 2013), which may contribute to age relationships with resting-state BOLD SD. Finally, the observed patterns may result from the general relationship between age and WMH. Thus, correcting for WMH may reduce age relationships with resting-state BOLD SD simply due to shared variance between these measures, rather than any mechanistic contribution of WMH-related changes. As a hypothetical example, one might expect a similar reduction in the age relationship if one controlled for bone density. Although the results are consistent with recent proposals that vascular influences may be an important factor in age-related cognitive decline (for review, see Abdelkarim et al. 2019; Wåhlin and Nyberg 2019), future studies should further examine resting-state BOLD variability using methods that allow for more mechanistic insight into the vascular contributions on the BOLD signal, including measures of cerebral blood flow and cerebrovascular reactivity.

Additionally, it might be informative to study relationships with white matter integrity using diffusion tensor imaging. Previous studies have demonstrated relationships between white matter integrity and resting-state BOLD variability in studies of cognition and physical activity in older adults (Burzynska, Wong, Voss, Cooke, Gothe, et al. (2015), Burzynska, Wong, Voss, Cooke, McAuley, et al. (2015)). Future studies should consider whether white matter integrity contributes to age-related differences in resting-state BOLD variability.

Conclusions

Our results replicate previous demonstrations that resting-state BOLD variability is negatively associated with age differences. We also demonstrate that if uncorrected by conservative preprocessing, head motion may positively bias estimates of resting-state BOLD variability. Moreover, age-related differences in resting-state BOLD variability may be sensitive to anatomically diffuse mechanisms, possibly related to WMH pathology, although our results do not suggest that these relationships are sensitive to CVH in general. Hence, the potential influence of motion, global signal artifacts, and WMH burden should be considered when processing, analyzing, and interpreting estimates of resting-state BOLD variability.

Overall, these results support the proposal that variability in the resting-state fMRI BOLD signal may reflect a sensitive signal that declines in older adulthood. It appears that WMH burden strongly modulates this relationship. As a speculation, the role of WMHs in the age-variability relationship could simply be due to damage to neural tissue that connects distinct areas of functional activity. However, vascular mechanisms might also be possible, as WMH has previously been shown to relate to cerebrovascular impairments, including greater pulsatility (Mok et al. 2012; Purkayastha et al. 2014) and arterial stiffness (Poels et al. 2012). Independent of the precise mechanism, it appears that estimates of resting-state BOLD variability might afford reliable, potentially clinically relevant biomarkers of age-related decline. The network-based, machine learning approach outlined in the present report might offer methods to maximize the sensitivity of these measures in future evaluations.

Supplementary Material

Supplementary material can be found at *Cerebral Cortex* online.

Funding

National Institutes of Health (grant numbers P01-AG026276, P01-AG03991, P50-AG05681, R01-AG052550, R01-AG057680, T32-AG000030–41, 1S10RR022984-01A1, 1S10OD018091–01, K01 AG053474), with generous support from the Paula and Rodger O. Riney Fund and the Daniel J. Brennan MD Fund.

Notes

We thank the participants for their dedication to this project, the Psychometric Core for psychometric test data, Doug Garrett for helpful comments, Jo Etzel for consultation on support vector regression analyses, Dimitre Tomov for technical and programming support, and Julie Wisch for data curation support. *Conflict of Interests*: The authors declare no competing interests.

References

Abdelkarim D, Zhao Y, Turner MP, Sivakolundu DK, Lu H, Rypma B. 2019. A neural-vascular complex of age-related changes in the human brain: anatomy, physiology, and implications for neurocognitive aging. *Neurosci Biobehav Rev*. 107:927–944.

Alfaro FJ, Gavrieli A, Saade-Lemus P, Lioutas VA, Upadhyay J, Novak V. 2018. White matter microstructure and cognitive decline in metabolic syndrome: a review of diffusion tensor imaging. *Metabolism*. 78:52–68.

Armitage SG. 1946. An analysis of certain psychological tests use for the evaluation of brain injury. *Psychol Monogr*. 60:1–48. doi: 10.1037/h0093567.

Aschenbrenner AJ, Gordon BA, Benzinger TLS, Morris JC, Hassenstab JJ. 2018. Influence of tau PET, amyloid PET, and hippocampal volume on cognition in Alzheimer disease. *Neurology*. 91:e859–e866.

Backman L, Nyberg LH, Lindenberger U, Li SC, Farde L. 2006. The correlative triad among aging, dopamine, and cognition: current status and future prospects. *Neurosci Biobehav Rev*. 30:791–807.

Betzel RF, Byrge L, He Y, Goñi J, Zuo X-N, Sporns O. 2014. Changes in structural and functional connectivity among resting-state networks across the human lifespan. *Neuroimage*. 102:345–357.

Brier MR, Thomas JB, Snyder AZ, Benzinger TLS, Zhang D, Raichle ME, Holtzman DM, Morris JC, Ances BM. 2012. Loss of intranetwork and internetwork resting state functional connections with Alzheimer's disease progression. *J Neurosci*. 32:8890–8899.

Burzynska AZ, Wong CN, Voss MW, Cooke GE, Gothe NP, Fanning J, McAuley E, Kramer AF. 2015a. Physical activity is linked to greater moment-to-moment variability in spontaneous brain activity in older adults. *PLoS One*. 10:1–18.

Burzynska AZ, Wong CN, Voss MW, Cooke GE, McAuley E, Kramer AF. 2015b. White matter integrity supports BOLD signal variability and cognitive performance in the aging human brain. *PLoS One*. 10:1–17.

Chan MY, Park DC, Savalia NK, Petersen SE, Wig GS. 2014. Decreased segregation of brain systems across the healthy adult lifespan. *Proc Natl Acad Sci USA*. 111:E4997–E5006.

Ciric R, Wolf DH, Power JD, Roalf DR, Baum GL, Ruparel K, Shinohara RT, Elliott MA, Eickhoff SB, Davatzikos C *et al*. 2017. Benchmarking of participant-level confound regression strategies for the control of motion artifact in studies of functional connectivity. *Neuroimage*. 154:174–187.

Cole JH, Franke K. 2017. Predicting age using neuroimaging: innovative brain ageing biomarkers. *Trends Neurosci*. 40:681–690.

Deco G, Jirsa VK, McIntosh AR. 2011. Emerging concepts for the dynamical organization of resting-state activity in the brain. *Nat Rev Neurosci*. 12:43–56.

Dosenbach NUF, Nardos B, Cohen AL, Fair DA, Power JD, Church JA, Nelson SM, Wig GS, Vogel AC, Lessov-schlaggar CN *et al*. 2010. Prediction of individual brain maturity using fMRI. *Science*. 329:1358–1361.

Filippi M, Rocca MA, De Stefano N, Enzinger C, Fischer E, Horsfield MA, Inglese M, Pelletier D, Comi G. 2011. Magnetic resonance techniques in multiple sclerosis: the present and the future. *Neurol Rev*. 68:1514–1520.

Fischl B. 2012. FreeSurfer. *Neuroimage*. 62:774–781.

Fox MD, Raichle ME. 2007. Spontaneous fluctuations in brain activity observed with functional magnetic resonance imaging. *Nat Rev Neurosci*. 8:700–711.

Fox MD, Zhang D, Snyder AZ, Raichle ME. 2009. The global signal and observed anticorrelated resting state brain networks. *J Neurophysiol*. 101:3270–3283.

Garrett DD, Kovacevic N, McIntosh AR, Grady CL. 2010. Blood oxygen level-dependent signal variability is more than just noise. *J Neurosci*. 30:4914–4921.

Garrett DD, Kovacevic N, McIntosh AR, Grady CL. 2011. The importance of being variable. *J Neurosci*. 31:4496–4503.

Garrett DD, Kovacevic N, McIntosh AR, Grady CL. 2013. The modulation of BOLD variability between cognitive states varies by age and processing speed. *Cereb Cortex*. 23:684–693.

Garrett DD, Lindenberger U, Hoge RD, Gauthier CJ. 2017. Age differences in brain signal variability are robust to multiple vascular controls. *Sci Rep*. 7:1–13.

Garrett DD, McIntosh AR, Grady CL. 2014. Brain signal variability is parametrically modifiable. *Cereb Cortex*. 24:2931–2940.

Garrett DD, Nagel IE, Preuschhof C, Burzynska AZ, Marchner J, Wiegert S, Jungehülsing GJ, Nyberg LH, Villringer A, Li S-C *et al*. 2015. Amphetamine modulates brain signal variability and working memory in younger and older adults. *Proc Natl Acad Sci U S A*. 112:7593–7598.

Garrett DD, Samanez-Larkin GR, MacDonald SWS, Lindenberger U, McIntosh AR, Grady CL. 2013. Moment-to-moment brain signal variability: a next frontier in human brain mapping? *Neurosci Biobehav Rev*. 37:610–624.

Geerligs L, Tsvetanov KA, Henson RN. 2017. Challenges in measuring individual differences in functional connectivity using fMRI: the case of healthy aging. *Hum Brain Mapp*. 38:4125–4156.

Goodglass H, Kaplan E. 1983. *Boston Diagnostic Aphasia Examination Booklet, III: Oral Expression: Animal Naming (Fluency in Controlled Association)*. Philadelphia: Lea and Febiger.

Gordon EM, Laumann TO, Adeyemo B, Huckins JF, Kelley WM, Petersen SE. 2016. Generation and evaluation of a cortical area parcellation from resting-state correlations. *Cereb Cortex*. 26:288–303.

Grady CL, Garrett DD. 2014. Understanding variability in the BOLD signal and why it matters for aging. *Brain Imaging Behav*. 8:274–283.

Grady CL, Garrett DD. 2018. Brain signal variability is modulated as a function of internal and external demand in younger and older adults. *Neuroimage*. 169:510–523.

Grober E, Buschke H, Crystal H, Bang S, Dresner R. 1988. Screening for dementia by memory testing. *Neurology*. 38: 900–903.

Guitart-Masip M, Salami A, Garrett DD, Rieckmann A, Lindenberger U, Bäckman L. 2016. BOLD variability is related to dopaminergic neurotransmission and cognitive aging. *Cereb Cortex*. 26:2074–2083.

Honey CJ, Kötter R, Breakspear M, Sporns O. 2007. Network structure of cerebral cortex shapes functional connectivity on multiple time scales. *Proc Natl Acad Sci*. 104:10240–10245.

Hu S, Chao HHA, Zhang S, Ide JS, Li CSR. 2014. Changes in cerebral morphometry and amplitude of low-frequency fluctuations of BOLD signals during healthy aging: correlation with inhibitory control. *Brain Struct Funct*. 219:983–994.

Kielar A, Deschamps T, Chu RKO, Jokel R, Khatamian YB, Chen JJ, Meltzer JA. 2016. Identifying dysfunctional cortex: dissociable effects of stroke and aging on resting state dynamics in MEG and fmri. *Front Aging Neurosci*. 8:1–22.

Krishnan A, Williams LJ, McIntosh AR, Abdi H. 2011. Partial least squares (PLS) methods for neuroimaging: a tutorial and review. *Neuroimage*. 56:455–475.

Marquez De La Plata C, Ardelean A, Koovakkattu D, Srinivasan P, Miller A, Phuong V, Harper C, Moore C, Whittemore A, Madden C *et al*. 2007. Magnetic resonance imaging of diffuse axonal injury: quantitative assessment of white matter lesion volume. *J Neurotrauma*. 24:591–598.

Mennes M, Zuo X-N, Kelly C, Di Martino A, Zang YF, Biswal BB, Castellanos FX, Milham MP. 2011. Linking inter-individual differences in neural activation and behavior to intrinsic brain dynamics. *Neuroimage*. 54:2950–2959.

Meyer D, Dimitriadou E, Hornik K, Weingessel A, Leisch F, Chang C-C, Lin C-C. 2017. Misc functions of the Department of Statistics, Probability Theory Group (formerly: E1071), TUWien. *Compr R Arch Netw*.

Mok V, Ding D, Fu J, Xiong Y, Chu WWC, Wang D, Abrigo JM, Yang J, Wong A, Zhao Q *et al*. 2012. Transcranial doppler ultrasound for screening cerebral small vessel disease: a community study. *Stroke*. 43:2791–2793.

Morris JC. 1993. The clinical dementia rating (CDR): current version and scoring rules. *Neurology*. 43:2412–2414.

Nielsen AN, Barch DM, Petersen SE, Schlaggar BL, Greene DJ. in press. Machine learning with neuroimaging: evaluating its applications in psychiatry. *Biol Psychiatry Cogn Neurosci Neuroimaging*.

Nielsen AN, Greene DJ, Gratton C, Dosenbach NUF, Petersen SE, Schlaggar BL. 2019. Evaluating the prediction of brain maturity from functional connectivity after motion artifact Denoising. *Cereb Cortex*. 29:2455–2469.

Nomi JS, Bolt TS, Ezie CEC, Uddin LQ, Heller AS. 2017. Moment-to-moment BOLD signal variability reflects regional changes in neural flexibility across the lifespan. *J Neurosci*. 37: 5539–5548.

Pantoni L. 2010. Cerebral small vessel disease: from pathogenesis and clinical characteristics to therapeutic challenges. *Lancet Neurol*. 9:689–701.

Poels MMF, Zaccai K, Verwoert GC, Vernooij MW, Hofman A, Van Der Lugt A, Witteman JCM, Breteler MMB, Mattace-Raso FUS, Ikram MA. 2012. Arterial stiffness and cerebral small vessel disease: the Rotterdam scan study. *Stroke*. 43:2637–2642.

Power JD, Barnes KA, Snyder AZ, Schlaggar BL, Petersen SE. 2012. Spurious but systematic correlations in functional connectivity MRI networks arise from subject motion. *Neuroimage*. 59:2142–2154.

Power JD, Cohen AL, Nelson SM, Wig GS, Barnes KA, Church JA, Vogel AC, Laumann TO, Miezin FM, Schlaggar BL *et al*. 2011. Functional Network Organization of the Human Brain. *Neuron*. 72:665–678.

Power JD, Mitra A, Laumann TO, Snyder AZ, Schlaggar BL, Petersen SE. 2014. Methods to detect, characterize, and remove motion artifact in resting state fMRI. *Neuroimage*. 84:320–341.

Power JD, Plitt M, Laumann TO, Martin A. 2017. Sources and implications of whole-brain fMRI signals in humans. *Neuroimage*. 146:609–625.

Power JD, Schlaggar BL, Petersen SE. 2015. Recent progress and outstanding issues in motion correction in resting state fMRI. *Neuroimage*. 105:536–551.

Purkayastha S, Fadar O, Mehregan A, Salat DH, Moscufo N, Meier DS, Guttmann CRG, Fisher NDL, Lipsitz LA, Sorond FA. 2014. Impaired cerebrovascular hemodynamics are associated with cerebral white matter damage. *J Cereb Blood Flow Metab*. 34:228–234.

Satterthwaite TD, Wolf DH, Loughead J, Ruparel K, Elliott MA, Hakonarson H, Gur RC, Gur RE. 2012. Impact of in-scanner head motion on multiple measures of functional connectivity: relevance for studies of neurodevelopment in youth. *Neuroimage*. 60:623–632.

Scarapicchia V, Garcia-barrera M, Macdonald S, Gawryluk JR. 2019. Resting state BOLD variability is linked to white matter vascular burden in healthy aging but not in older adults with subjective cognitive decline. *Front Hum Neurosci*. 13: 1–13.

Scarapicchia V, Mazerolle EL, Fisk JD, Ritchie LJ, Gawryluk JR. 2018. Resting state BOLD variability in Alzheimer's disease: a marker of cognitive decline or cerebrovascular status? *Front Aging Neurosci*. 10:1–13.

Schmidt P, Gaser C, Arsic M, Buck D, Förschler A, Berthele A, Hoshi M, Ilg R, Schmid VJ, Zimmer C *et al*. 2012. An automated tool for detection of FLAIR-hyperintense white-matter lesions in multiple sclerosis. *Neuroimage*. 59:3774–3783.

Schmidt R, Fazekas F, Kapeller P, Schmidt H, Hartung HP. 1999. MRI white matter hyperintensities: three-year follow-up of the Austrian stroke prevention study. *Neurology*. 53: 132–139.

Seitzman BA, Gratton C, Marek S, Raut RV, Dosenbach NUF, Schlaggar BL, Petersen SE, Greene DJ. 2020. A set of functionally-defined brain regions with improved representation of the subcortex and cerebellum. *Neuroimage*. 206: 1–17.

Shulman GL, Pope DLW, Astafiev SV, McAvoy MP, Snyder AZ, Corbetta M. 2010. Right hemisphere dominance during spatial selective attention and target detection occurs outside the dorsal frontoparietal network. *J Neurosci*. 30: 3640–3651.

Tsvetanov KA, Henson RN, Jones PS, Mutsaerts H-J, Fuhrmann D, Tyler LK, Cam-CAN, Rowe JB. 2019. The effects of age on resting-state BOLD signal variability is explained by cardiovascular and neurovascular factors. *bioRxiv*. preprint. 836619. doi: 10.1101/836619.

Tsvetanov KA, Henson RNA, Tyler LK, Davis SW, Shafto MA, Taylor JR, Williams N, Rowe JB. 2015. The effect of ageing on fMRI: correction for the confounding effects of vascular reactivity evaluated by joint fMRI and MEG in 335 adults. *Hum Brain Mapp*. 36:2248–2269.

Van Dijk KRA, Sabuncu MR, Buckner RL. 2012. The influence of head motion on intrinsic functional connectivity MRI. *Neuroimage*. 59:431–438.

Wåhlin A, Nyberg L. 2019. At the heart of cognitive functioning in aging. *Trends Cogn Sci*. 23:717–720.

Wardlaw JM, Smith EE, Biessels GJ, Cordonnier C, Fazekas F, Frayne R, Lindley RI, O'Brien JT, Barkhof F, Benavente OR *et al*. 2013. Neuroimaging standards for research into small vessel disease and its contribution to ageing and neurodegeneration. *Lancet Neurol*. 12:822–838.

Wig GS, Schlaggar BL, Petersen SE. 2011. Concepts and principles in the analysis of brain networks. *Ann N Y Acad Sci*. 1224:126–146.

Yarkoni T, Westfall J. 2017. Choosing prediction over explanation in psychology: lessons from machine learning. *Perspect Psychol Sci*. 12:1100–1122.

Yeo BTT, Krienen FM, Sepulcre J, Sabuncu MR, Lashkari D, Hollinshead M, Roffman JL, Smoller JW, Zöllei L, Polimeni JR *et al*. 2011. The organization of the human cerebral cortex estimated by intrinsic functional connectivity. *J Neurophysiol*. 106:1125–1165.